Insect Biochemistry and Molecular Biology 110 (2019) 69–79

Contents lists available at ScienceDirect

Insect Biochemistry and Molecular Biology

journal homepage: www.elsevier.com/locate/ibmb

Manduca sexta Perilipin 1B: A new PLIN1 isoform linked to fat storage prior to pupation

Xiao Chen, Sarah J. Firdaus, Zhiyan Fu, Zengying Wu, Jose L. Soulages, Estela L. Arrese*

Department of Biochemistry and Molecular Biology, Oklahoma State University, Stillwater, OK, 74078, USA

ARTICLE INFO

Keywords:
PLIN1
LSD1
Lipid droplets
Triacylglycerol
Triglycerides
Fat body
Manduca sexta

ABSTRACT

Perilipins (PLINs) are proteins that associate with lipid droplets (LDs) and play roles in the control of triglycerides (TG) metabolism. Two types of PLINs - 1 and 2- occur in insects. Following previous work on MsPLIN1A (a 42 kDa protein formerly called MsLsd1), here we report a new PLIN1 isoform, MsPLIN1B. MsPLIN1B cDNA was cloned and the 1835bp cDNA contains an ORF encoding a 47.9 kDa protein whose expression was confirmed by mass spectrometry. Alternative transcripts A and B, which differ in the alternative use of exon 1, were the most abundant PLIN1 transcripts in the fat body. These transcripts encode nearly identical proteins except that the B isoform contains 59 additional residues in its amino terminus. No conserved domain was identified in the extra region of MsPLIN1B. The novel PLIN1 isoform is found in lepidopteran species. In *Manduca*, PLIN1B was expressed only in the 5th instar larva and its levels correlated with fat storage. Furthermore, PLIN1B levels increased with the fat content of the diet in insects of the same age confirming a direct relationship between PLIN1B and TG storage irrespective of development. The nutritional status impacted PLIN1B levels, which decreased in starvation and increased with subsequent re-feeding. Altogether data support a link between PLIN1B and TG storage in caterpillars prior to pupation. The combined findings suggest distinct roles for PLIN1A, PLIN1B and PLIN2. MsPLIN1A abundance correlates with mobilization of TG stores, MsPLIN2 with the synthesis of new LDs and MsPLIN1B abundance correlates with high levels of TG storage and large LD sizes at the end of the last feeding period.

1. Introduction

Insects store excess nutrients as fat (triglycerides, TG) and glycogen in the fat body. Fat reserves are essential for insect growth, development and oogenesis. During vitellogenesis, fat reserves are mobilized to the ovaries for egg development (Law and Wells, 1989). Moreover, TG are crucial to meet the energy demands during diapause and prolonged periods of flight due to the high caloric content per unit of weight. TG are the storage form of fatty acids (FA). FA have important physiological functions as components of cell membranes, cuticular lipids, waxes as well as precursors in the synthesis of lipid regulators and hormones in addition of being a source of energy (Canavoso et al., 2001). Clearly TG reserves are essential to support the life of insects, and fat is always a major component of the fat body (Arrese and Soulages, 2010). During periods of food abundance, TG are deposited in the fat body cell as cytoplasmic lipid droplets (LDs). LDs are globular organelles consisting of a lipid core (TG and cholesterol ester) surrounded by a monolayer of phospholipids and a coat of proteins (Bickel et al., 2009; Brasaemle, 2007). When the organism needs energy, stored fatty acids are mobilized from TG by hydrolysis (lipolysis) catalyzed by lipases. In turn, fatty acids can be used for ATP production through β-oxidation or secreted to circulation as diglycerides (DG) to be transported by lipophorin to other organs (Van der Horst and Rodenburg, 2010).

LDs are dynamic organelles that can growth in size and number depending on the metabolic condition. The fate of LDs is controlled by the protein coat, which comprises many different proteins (Hodges and Wu, 2010). Proteomic studies of LDs isolated from insects, *Drosophila* (Cermelli et al., 2006; Beller et al., 2006) and *Manduca* (Soulages et al., 2012), have shown that LD proteins vary with the type of tissue and the developmental stage. However, all LD proteomes from numerous animals showed one or more members of the Perilipins or PAT proteins (Hodges and Wu, 2010). This group of proteins originally discovered in vertebrates is composed by PLIN1 (Perilipin), PLIN2 (ADRP), PLIN3 (TIP47), PLIN4 (S3-12) and PLIN5 (OXPAT) (Bickel et al., 2009). Insects display only two types of PLIN proteins: PLIN1 (Lsd1) and PLIN2 (Lsd2) (Lu et al., 2001; Miura et al., 2002). PLIN proteins have been implicated in TG metabolism and LD formation (Chen and Goodman,

* Corresponding author.
E-mail address: destela@okstate.edu (E.L. Arrese).

https://doi.org/10.1016/j.ibmb.2019.05.001
Received 8 January 2019; Received in revised form 1 May 2019; Accepted 1 May 2019
Available online 02 May 2019
0965-1748/

2017). The overall amino acid sequence conservation among PLIN proteins is very low, but they share a ~100 amino acids long region towards the N-terminus –the PAT domain-that is conserved (Lu et al., 2001). The importance of this domain remains enigmatic but is not required for binding to LDs (Najt et al., 2014). PLINs lack apparent transmembrane domains and they are thought to associate to LDs by regions of amphipatic helices (Brasaemle, 2007). The overall secondary structure of *Drosophila* PLIN1 is α helical, and the four helices clustered in the central part of the polypeptide were identified as the lipid binding elements to the surface of the LD (Arrese et al., 2008a).

PLIN1 is the best characterized member of the family (Sztalryd and Brasaemle, 2017). In the adipose tissue of vertebrates, PLIN1 plays a role in TG homeostasis as a regulator of lipid storage and lipolysis. PLIN1 dual roles are determined by its phosphorylation state. Under basal condition, unphosphorylated PLIN1 acts as a hydrolytic barrier preventing lipases from gaining access to TG (Brasaemle et al., 2000; Souza et al., 2002; Tansey et al., 2004). Under a high lipolytic condition typically triggered by hormones, PLIN1 becomes phosphorylated enabling directly or indirectly the action of major lipases (Brasaemle, 2007; Ducharme and Bickel, 2008). However, the manipulation of PLIN1 levels in mice showed the complexity of the physiological role of this protein. Although depletion of PLIN1 produced a decrease in TG storage supporting the barrier function of PLIN1 (Martinez-Bota et al., 2000; Tansey et al., 2001), overexpression of PLIN1 produced a decrease in both basal and stimulated lipolysis with reduced TG storage (Miyoshi et al., 2010).

In insects, PLIN1 has been associated with TG lipolysis in the fat body (Patel et al., 2005; Beller et al., 2010; Bi et al., 2012; Toprak et al., 2014), silkmoth sex pheromone biosynthesis (Ohnishi et al., 2011), and with proper wing development (Tran et al., 2017). In *Manduca*, AKH -the lipolytic hormone in the fat body of adults-triggers a two-fold increase in hemolymph lipid levels (Arrese and Wells, 1997). AKH stimulation induces PLIN1 (42 kDa) phosphorylation, which correlates with the activation of lipolysis (Patel et al., 2005). In vitro studies confirmed the effect of PLIN1 phosphorylation in the activation of purified triglyceride lipase TGL (Arrese et al., 2008a). Moreover, MsPLIN1 is more abundant in the fat body of adults, which present the highest level of lipolysis. Thus, the pattern of expression of MsPLIN1 during development was also consistent with a role of PLIN1 in lipid mobilization (Arrese et al., 2008b). Unlike vertebrate PLIN1, the depletion of PLIN1 in adult *Drosophila* induced an increase in TG storage suggesting also a role for DmPLIN1 in lipolysis (Beller et al., 2010). DmPLIN1 was also an effector of the AKH-lipolytic pathway (Grönke et al., 2007) involved in the activation of DmHSL (Bi et al., 2012). DmATGL or Brummer lipase is shielded by DmPLIN2 and DmPLIN1 in small lipid droplets (Grönke et al., 2003; Beller et al., 2010; Bi et al., 2012) while DmPLIN1 facilitates hormone sensitive lipase (HSL)-mediated lipolysis in large lipid droplets (Bi et al., 2012). The analysis of double PLIN mutants (plin1 and 2) in *Drosophila* showed that perilipins are dispensable for the formation of the small LDs, but are needed for subsequent LD growth (Bi et al., 2012). However, previously Beller et al. (2010) showed that LDs of different sizes including large droplets exist in fat body cells of mature adult Drosophila flies lacking both, PLIN1 and PLIN2. In *Manduca*, we found a relationship between PLIN2 expression and TG synthesis suggesting that PLIN2 is needed when fat body or midgut were accumulating TG. However, MsPLIN2 declined in the fat body of the 5th instar at the time of maximal TG storage. This unexpected finding suggested the occurrence of alternative mechanism/s to shield TG from the action of lipases in *M. sexta* LDs (Chen et al., 2017).

Here we report a new PLIN1 isoform of *M. sexta*, PLIN1B, which was identified as a 47.9 kDa LD-associated protein from the fat body of the 5th instar larva. Fifth instar larva embodies the final feeding period, during which caterpillars feed intensely and accumulate the greatest amounts of lipid reserves prior to pupation.

2. Materials and methods

2.1. Insect rearing and feeding

M. sexta eggs were purchased from Carolina Biological Supplies. Larvae were reared at 25 °C on artificial diet (Bell and Joachim, 1976) unless otherwise is indicated. The artificial diet is a mixture of dry components (20% w/v) in water (80% w/v). The main components of the dry mix are: wheat germ (72%), casein (14%), Wesson's salt mix (4.2%) and Vanderzant vitamin mixture (6.4%). Adult insects were maintained at room temperature. The end of the 4thinstar was identified by the appearance of head capsule (HC) slippage (day 0, 5th instar). Fifth instar larva were sorted by the number of days of feeding (day 1 to day 5). Subsequently, wanderers were identified by initiation of wandering behavior and the exposure of the dorsal aorta. Under these rearing conditions the feeding period of the 5th instar larva last 5 days and the pre-pupal period also last 5 days. *2.1.1. Starvation and re-feeding*: Second day 5th instar larvae were kept individually without diet for 24 h. Subsequently, starved insects were re-fed with diet (*ad libitum*). Fat bodies were collected at 0 h, 2 h, 6 h, and 48 h after re-feeding. *2.1.2. Feeding 5*th *instar larvae with diets of different caloric content:* Larvae were reared from hatching to the completion of the 4th instar on the artificial diet. From the beginning of the 5th instar, larvae were subjected to four types of diets: leaves (tomato leaves), leaves with oil (tomato leaves with the addition of 33 μl of corn oil per gram leaves), diet (artificial diet according to Bell and Joachim (1976)), and diet with oil (standard diet with the addition of 33 μl of corn oil per gram). Tomato leaves were harvest daily, rinsed with water, wrapped in paper towels and kept in a plastic bag at 4 °C. The oil was Wesson Corn Oil (100% corn oil) purchased at a local food store. The caloric content of the leaf diet was 0.13 kcal/g and 0.30 kcal/g of tomato leaves without and with oil, respectively, whereas for the artificial diet was 0.52 kcal/g and 0.69 kcal/g with oil. Each day animals were provided with increasing amounts of corresponding diet from 0.4 g (day 1) to 1.6 g (day 4) per insect. Fat bodies were dissected at various times during feeding for further analysis by Western blot, qPCR, TG measurements, and microscopy to determine lipid droplets size distribution.

2.2. PLIN1 developmental expression

Fat bodies from larva and adults were dissected along development for qPCR and Western blot. Fat bodies for qPCR analysis were processed as indicated below (section 2.5). Fat bodies for Western blot analysis were homogenized in homogenization buffer (HB) (20 mM Tris, pH 7.4, 0.25 M sucrose, 1 mM EDTA, 1 mM benzamidine, 1 mM PMSF, 10 mg/l leupeptine, 1 mM DTT) containing sucrose. Homogenates from at least a pool of two fat bodies were centrifuged at 1000 g for 10 min. The supernatant was overlaid with HB without sucrose and centrifuged at 160,000 g for 1 h. The thin white layer floating at the top (LDs) was collected and resuspended in HB buffer and the protein concentration was determined by Bradford's method (Sigma). Laemmli buffer (Sigma) was added to LDs samples used for SDS-PAGE for subsequent Western blot analysis as described in section 2.3.

2.2.1. Subcellular fractionation

Fat body homogenate was centrifuged at 1000 g for 10min and the resulting supernatant was adjusted to 1.17M sucrose and transferred to a SW40 centrifuge tube to be subsequently overlaid with 1 ml each of 1.02 M sucrose, 0.87 M sucrose, 0.58 M sucrose, 0.29 M sucrose, 0.15 M sucrose in HB buffer and 1.5 ml of buffer without sucrose. Density gradients were centrifuged at 160,000 g for 4 h and fractionated into ten fractions, which were analyzed by Western blot to determine the PLIN1 isoforms as described below (section 2.4). The concentration of triglycerides in each fraction was determined with the Infinity Triglycerides Reagent (section 7) and protein concentration was determined by Bradford's method (Sigma). Lipid droplets localized at the top

fraction. This fraction comprised 96.9 ± 1.1% and 3% of cellular triglycerides and proteins, respectively.

2.3. Cloning and sequencing of PLIN1A and B cDNAs

To clone the full-length cDNA of PLIN1A and PLIN1B, a cDNA library obtained from larval fat body and the following gene specific primers were used. PLIN1A-F: 5′- CAACGTATTGTGCGAAATGGTCAT AGC-3′ PLIN1B-F: 5′- CAACAGATTACATTATTTTTAACCGAGATAACC -3′ and common reverse primer PLIN1 R: 5′- GCTATTAAGCACAGGCT CTACATACGT- 3′ designed based on the sequence information from the *Manduca* genome were used in PCR experiments. Each PCR reaction produced a single band (~1.6 kb and 1.8 kb, respectively), which was cloned into pGEM vector (Novagen) and sequenced in both directions.

2.4. Preparation of polyclonal MsPLIN1 antibody and Western blot analysis

The coding region of PLIN1A was amplified by PCR and the PCR product was cloned into pET32-Ek/LIC vector (Novagen) and sequenced. *E. coli* strain NovaBlue GigaSingles cells (Novagen) were transformed with the recombinant plasmid. Positive clones were confirmed by DNA sequencing. *E coli* Rosetta 2 cells (Novagen) were transformed for protein expression. Expression of the recombinant protein was induced with 1 mM IPTG. After 4 h, bacteria were collected and resuspended in lysis buffer (50 mM Tris pH 8, 1 mM EDTA, 100 mM NaCl, 1 mM PMSF) containing 0.3 mg/ml of lysozyme. After 30min incubation, the preparation was centrifuged at 160,000 × *g* for 30min. The fusion protein was found in the pellet, which was resuspended in 20 mM Tris pH 8, 6M urea, 500 mM NaCl by sonication. After centrifugation (160,000 × *g*, 15 min), purification of recombinant PLIN1A was carried out essentially as previously reported (Arrese et al., 2008b). The fusion protein was cleaved by thrombin to remove the thioredoxin/His-tag portion. Purified PLIN1 was used to generate polyclonal antibodies in rabbit (Cocalico Biologicals Inc.). For Western blot analysis, proteins were separated by SDS-PAGE (Bio-Rad) and transferred to nitrocellulose membranes (Bio-Rad). The blots were developed with ECL chemiluminescence reagents (GE Healthcare) and exposure directly against X-ray films (Fisher). The abundance of PLIN1 was estimated by measuring the net band density on the X-ray films by AlphaEaseFC software (Innotech). Ponceau S staining of the membrane followed by densitometry was used to estimate the total amount of protein in each lane (Romero-Calvo et al., 2010).

2.5. LC-MS/MS

Lipid droplet proteins were subjected to SDS-PAGE in 4–20% acrylamide gradient gels (Novex, Invitrogen). Each lane of the Coomassie Blue stained gel was divided in six regions. Sections 3 and 4 covering 70-45 kDa and 45-30 kDa, respectively were analyzed for PLIN1 peptides. Each gel slice was finely minced. Proteins from each slice were reduced with tris(2-carboxyethyl)phosphine, alkylated with iodoacetamide, and digested for 6–16 h with 8 μg/ml trypsin, using 50 mM ammonium bicarbonate as buffer. Digestion products were analyzed by LC-MS/MS.

Samples were analyzed on a hybrid LTQ-Orbitrap XL mass spectrometer (Thermo Fisher Scientific) coupled to a New Objectives PV-550 nanoelectrospray ion source and an Eksigent NanoLC-2D chromatography system. Peptides were analyzed by trapping on a 2.5 cm ProteoPrepII pre-column (New Objective) and separation on a 75 μm ID fused silica column, packed in house with 10-cm of Magic C18 AQ, terminated with an integral fused silica emitter pulled in house. Peptides were eluted using a 5–40% ACN/0.1% formic acid gradient performed over 40 min at a flow rate of 300 nl/min. During each 1-s full-range FT-MS scan (nominal resolution of 60,000 FWHM, 300–2000 m/z), the three most intense ions were analyzed via MS/MS in the linear ion trap. MS/MS settings used a trigger threshold of 8000 counts, monoisotopic precursor selection, and rejection of parent ions that had unassigned charge states, were previously identified as contaminants on blank gradient runs, or were previously selected for MS/MS (data dependent acquisition using a dynamic exclusion for 150% of the observed chromatographic peak width). Column performance was monitored using trypsin autolysis fragments (m/z 421.76), and via blank injections between samples to assay for contamination. Data analysis: Centroided ion masses were extracted using the extract_msn.exe utility from Bioworks 3.3.1 and were used for database searching with Mascot v2.2.04 (Matrix Science) and X! Tandem v2007.01.01.1 (www.thegpm.org). A database containing the predicted proteins from all arthropods from NCBI was utilized for searching including the predicted PLIN1 sequences from the Manduca genome that were manually added into the data base. MASCOT was set up to search NCBI. Searches used a fragment ion mass tolerance of 0.80Da and a parent ion tolerance of 10.0 ppm. Searches included the following potential peptide modifications: pyroglutamate modification of N-terminal glutamines, oxidation of methionine, acrylamide, and iodoacetamide adducts of cysteine, as well as potential formylation and acetylation of the N-terminus of the parent protein. Scaffold (Proteome Software) was used to validate MS/MS-based peptide and protein identifications. Peptide identifications were accepted if they could be established at greater than 99.9% probability as specified by the Peptide Prophet algorithm.

2.6. Real time quantitative PCR (RT-qPCR)

Total RNA was extracted from a pool of at least two fat bodies using Trizol reagent (Invitrogen). cDNA was synthesized from 1.0 μg total RNA using iScript cDNA synthesis Kit (Bio-Rad) following manufacturer's instructions. Quantitative real-time PCR (qPCR) was carried out using iTaq Universal SYBR Green Supermix (Bio-Rad) and CFX Connect Real-Time PCR Detection System (Bio-Rad) in 10 μl reactions. The PCR reaction conditions were initial denaturation at 95 °C for 1 min, followed by 45 cycles alternating denaturation at 95 °C for 2s and annealing/extension at 60 °C for 45s. PLIN1A (5′-GTTCCATCTCAGTACA CAGCTCCGA-3′ and 5′-AGAGTCCGGCATTGGTGTCACAG-3′) and PLIN1B (5′-GAAGAACAAACTCTGCCGCACTC-3′ and 5′-ACGTCACCAT TTCCCGCCATC-3′) specific primers were used in corresponding reactions. In addition, total PLIN1 expression was assessed using specific primers for an internal region common to both transcripts (5′- TAGAC AGGCGCTCGCTGAGG-3' (exon 5) and 5′- TCTGGCTCCGGCTGGCT AAG-3' (exon 6)). Expression of each transcript was normalized using the ribosomal protein S3 (5′-TACAAACTCATTGGAGGTCTGGCCGT-3′ and 5′- ACGAACTTCATGGACTTGGCTCTC-3′) as an internal control (reference). DGAT expression was assessed using the following specific primers: 5′-CTTGTTGGCCCCTACTCTATGTTACGA-3′ and 5′- GTCACT GAGGGTATCATCCATTGCTG-3'. At least two independent sets of total RNA were analyzed in triplicate. Relative values are plotted as the mean ± SD. The amplification efficiency of each primer pair for the target and reference (rpS3) genes were determined in separate RT-PCR experiments in which amplifications of serial dilutions of cDNA were performed. Primer pairs having very close amplification efficiency to the reference were acceptable to use to determine the relative gene expression by RT-qPCR. The similarity in the amplification efficiency was judged by the slope of the plot of log cDNA dilution versus ΔC_T. A slope very close to zero was considered acceptable (Livak and Schmittgen, 2001).

2.7. Lipid measurement

Total lipids were extracted from tissue with chloroform-methanol (Folch et al., 1957) and analyzed for TG content using the Infinity Triglycerides Reagent (Thermo) as previously described (Chen et al., 2017). Briefly, lipid extracts were dried under air and resuspended in phosphate buffer saline (pH 7.4) containing 0.05% (v/v) of reduced Triton X-100. Fifteen microliter aliquots were used for lipid

determinations, which were performed by duplicate using triolein as standard.

2.8. Lipid droplets size distribution

Fat bodies were collected from 5th instar larvae fed on artificial diet or leaves with and without oil supplementation (see section 2.1.3.). The tissue was fixed, sectioned and analyzed in a Leica SP2 laser scanning confocal microscope using the transmitted light detector mode as described previously (Chen et al., 2017). To determine LD sizes, a total count of LDs ranging from 139 to 202 for each sample was used. LD sizes were clustered in two classes (small and large) according to their diameters (≤5 μm and > 5.5 μm). The LD count for each class size was estimated as well as the average percentage of LD counts and their corresponding SD. For each feeding group (A, leaf; B, leaf plus oil; C, diet; and D, diet plus oil), the mean values for "small (≤5 μm)" and "large (> 5.5 μm)" LDs were compared by the Student t-test.

3. Results

3.1. Identification of new PLIN1 isoform in 5th instar larval fat body

The complete development of *M. sexta* consists of several stages including embryo, five larval (1st to 5th instar) stages, wandering (prepupal), pupal and adult stages (Fig. 1S). The tobacco hornworm grows in the lab to a weight of over 10 g on an artificial diet. 90% of the growth in *Manduca* takes place in the 5th larval instar (Nijhout et al., 2006).

A previous report identified PLIN1 (formerly called Lsd1) as a ~42 kDa protein associated with the lipid droplets of the fat body from adults of *M. sexta* (Patel et al., 2005). The protein is more abundant in the fat body of adults and was originally undetected by Western blot in the fat body of larvae (Arrese et al., 2008b; Soulages et al., 2012). Subsequent mass spectrometry analysis of LD-associated proteins identified PLIN1 in the fat body of the 5th instar larvae (Soulages et al., 2012). Here, we re-investigated the expression of PLIN1 in the fat body of *M. sexta* during larval development by immunoblot using antibodies raised against the recombinant protein. PLIN1 (42 kDa) was detected in LDs from all developmental stages, including larva of the 3rd, 4th and 5thinstar and adults (Fig. 1, band labeled "A"). PLIN1 was detected in LD isolated from embryo and whole body homogenates of 1st and 2nd instar larvae but it was undetected in the ovaries (Fig. 1). A second band ("B") of 47–49 kDa was also detected in the fat body of the last (5th) instar larva (Fig. 1).

The subcellular localization of PLIN1 in the 5th instar fat body was studied by immunoblot of the subcellular fractions obtained by ultracentrifugation in sucrose gradient. Immunoblot analysis of the subcellular fractions showed that the 47–49 kDa protein was detected at the top of the of the sucrose gradient (fraction 1, 0% sucrose) (Fig. 2). The vast majority (> 95%) of cellular triglycerides (TG) localized in fraction 1 indicating the presence of the majority of lipid droplets in this fraction, which also contained ~ 3% of the proteins. These results indicated that the majority of lipid droplets and PLIN1 were localized at the top of the sucrose gradient.

Altogether, the data shown in Figs. 1 and 2 suggested the presence of a new MsPLIN1 isoform in the fat body of the 5th instar.

3.2. Cloning of M. sexta PLIN1 cDNA sequences and PLIN1 gene organization

We examined the occurrence of PLIN1 isoforms in the newly available *Manduca* genome that has been recently sequenced and assembled (Kanost et al., 2016). PLIN1 gene is a single copy gene containing 10 predicted exons and several possible transcripts. The prevalence of PLIN1 transcripts in the fat body of larva and adults was assessed by PCR and RT-PCR (data not shown). Variants A and B were

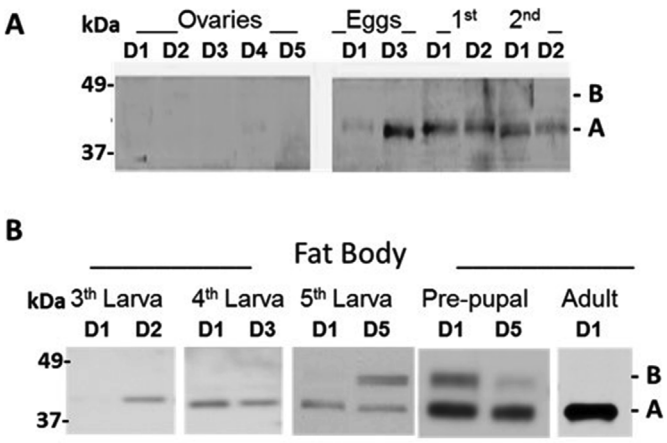

Fig. 1. Protein expression of *M. sexta* PLIN1 during development analyzed by Western blot using MsPLIN1 antibodies. Panel A): PLIN1 occurrence in the ovaries of virgin females (days 1–5), eggs (days 1 and 3), whole body homogenates of 1st (day 1 and 2) and 2nd stage (day 1 and 2) larva; **Panel B**): fat bodies of 3rd (day 1–2), 4th (day 1 and 3) and 5th instar (day 1 and 5) larvae and adult insects (day 1). Lipid droplets proteins (~20 μg) were loaded in each gel lane. PLIN1 is the 42 kDa band ("A"). A second band of ~47 kDa ("B") was detected in the 5th instar D5 fat body. A schematic representation of the *Manduca* life cycle including the duration of each stage in days is shown in Fig. 1S.

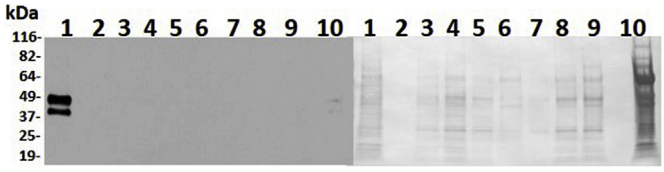

Fig. 2. Subcellular distribution of MsPLIN1. Fat body homogenate from 5th instar larvae (day 5) was subjected to ultracentrifugation in a sucrose gradient. The gradient was fractionated into ten fractions. Proteins from each fraction were separated by 4–20% SDS-PAGE and analyzed by Western blot using MsPLIN1 antibodies. Lanes were loaded with 1% of the total protein for all fractions, but fraction 10 (0.5%). Left panel: Western blot showing PLIN1 "A" and "B" bands in lane 1. Right panel: Ponceau S staining of the membrane used in the Western blot.

the predominant forms detected in larva fat body whereas in the fat body of adults PLIN1A was the main variant (see 3.3). The cDNA for PLIN1 A and PLIN1 B was cloned and sequenced as indicated in Material and Methods. PLIN1A cDNA (1602bp) and PLIN1B cDNA (1835bp) sequences were deposited in GenBank (accession KF835603.1 and KF835604.1). The ORF in PLIN1B cDNA localizes between positions 123–1421 and the molecular mass of translate is 47.9 kDa (Fig. 2S). In PLIN1A, the ORF localizes between positions 51–1184 and the corresponding translate has a molecular mass of 41.8 kDa. The two cDNA sequences were 99.2% identical in a 1523 nt overlap extending from nucleotides 52 to 1574 and 325 to 1835 in A and B isoforms, respectively. Thus, the main difference between the two sequences was in the 5′ region. The 3′-UTR (415bp) region is in common to both transcripts (Fig. 4S A-B). Three copies of predicted poly-adenylation signaling sites, AATAA, were identified in the 3′-UTR region (Figs. 2S and 4S A-B).

The MsLsd1 clone (1704 bp) previously identified (accession number EU809925.1, Arrese et al., 2008a) is an incomplete sequence of PLIN1B. The cDNA sequence (1835bp, Fig. 3S A-B) cloned in this work (KF835604.1) has an additional stretch to the 5′end that was missing in the EU809925.1 clone previously reported (Arrese et al., 2008b). The name Lsd1 was changed to PLIN1 following the recommendation by Kimmel et al. (2010).

PLIN1A and B proteins are nearly identical except that the B isoform

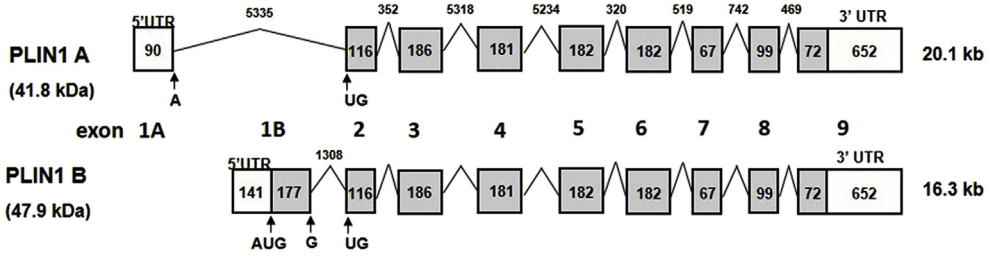

Fig. 3. Gene structure of *M. sexta* PLIN1 A and PLIN1 B. *M. sexta* PLIN1 genomic information was obtained from the Manduca genome (http://agripestbase.org/manduca/). Exons, introns, 5′-UTR and 3′-UTR are shown with grey boxes, lines, and white boxes, respectively. The initiation codons of the PLIN1 are pointed with arrows. Length of the exons and introns is indicated by number of nucleotides (nt).

contains 59 additional residues at its amino terminus (1–59) (Fig. 5). The occurrence of PLIN1B was confirmed by mass spectrometry of LD proteins from larval and adult fat bodies. PLIN1B peptides unique to this isoform were found in LDs from larval fat body (Figs. 2S and 6S A). Several peptides matching the N-term region (48% coverage in the unique 60 amino acids long region) of PLIN1B were detected. On the other hand, MS/MS analysis of LD protein isolated from adult fat body did not identify any of the aforementioned peptides (Fig. 6S B).

Fig. 3 shows the structure of MsPLIN1 gene deduced from the information provided in the *Manduca* genome and the cDNA sequences obtained in this study. The gene spans ~20 kb and contains 10 exons (Kanost et al., 2016). Exon 1B is located in the intron downstream of exon 1A. The usage of two alternative promoters would lead to different transcription start sites and to the expression of two alternative transcripts (A and B). There is no information on the promoter regions so far. The two transcripts differ in the 5' end as a result of the differential use of exon 1A or 1B. The predicted coding exons shown in Fig. 4 encode nearly identical proteins except that exon 1B transcript encodes additional residues. Exon 1B encodes an N terminal extension of 59 amino acids (Fig. 3). Residue 60 of PLIN1B is Val and the codon (GUG) originates at the joint of exon 1B and exon 2 (the last nucleotide of exon 1B is G and the first two nucleotides of exon 2 are UG). PLIN1A transcript uses exon 1A. In exon 1A transcript, the first nucleotide (A) of the start codon (AUG) is in exon 1A whereas the second and third nucleotides (UG) are in exon 2 (Fig. 3). The N term of PLIN1A translate is ^{1}MTRSQKPNMPR^{11} whereas the equivalent sequence of translate B is ^{60}VTRSQKPNMPR^{70}. After the methionine at position 1 in PLIN1A or the valine residue at position 60 in PLIN1B the amino acid sequence of both translates is identical.

The predicted sequence of PLIN1A deposited in GenBank (AIE17453.1) contains a short sequence "^{163}VIIV^{166}". This short sequence is missing in the PLIN1B sequence that we deposited in GenBank (AIE17454.1) (Fig. 5S). However, further work showed some PLIN1B clones encoded the predicted VIIV sequence (^{222}VIIV^{225} in PLIN1B). The short sequence is not associated with one of the predicted exons shown in Fig. 3. The sequence could arise in the splicing between exons 4 and 5 (Fig. 3S A). Additional work is required to elucidate this issue.

Multiple sequence alignment of all insect PLIN1 proteins available revealed that the extra 59 amino acids region at the N term of MsPLIN1B only aligned with predicted PLIN1 proteins from lepidopteran insects including the silkworm *(Bombyx mori),* the monarch butterfly (*Danaus plexippus*), the diamondback moth *(Plutella xylostella)*, the cotton leafworm (*Spodoptera litura*), the corn earworm (*Helicoverpa armigera*), the navel orangeworm (*Amyelosis transitella*), the chinese yellow swallowtail (*Papilio xuthus*), among other species. As an example, Fig. 5 A shows the sequence alignments of PLIN1 proteins from *Manduca sexta*, Ms; *Bombyx mori,* Bm; *Danaus plexippus*, Dp; and the dipteran *Drosophila melanogaster*, Dm. *Drosophila* genome predicts three PLIN1 isoforms (Gramates et al., 2017) but none of them displays the extra region present in MsPLIN1B. Moreover, no vertebrate PLIN protein sequence aligned with the additional sequence of PLIN1B.

Given that the PAT domain of PLIN proteins localizes towards the N term, we wondered if the extra region of 59 amino acids of PLIN1B was a PAT domain. However, detailed analysis of the sequence including sequence alignment of 22 insect PLIN proteins and 8 vertebrates PAT proteins (Lu et al., 2001) failed to identify a conserved domain in the extra region at the N term of PLIN1 B. MsPLIN1B showed a single PAT domain, which extends from amino acids 73 to 160 (Fig. 4 A). Therefore, both isoforms A and B shared identical PAT domains.

The most conserved sequence of insect PLIN1 proteins is in the central region of the protein, Fig. 4B. This region, which is comprised between amino acids 272 to 337 of MsPLIN1B, contains the predicted lipid binding elements and the highly conserved segment, ^{304}EPENQARP^{311}, previously recognized as a putative lipase interacting motif (Arrese et al., 2008a; Lin et al., 2014).

3.3. Developmental changes in PLIN1 mRNA levels in the fat body of M. sexta

Fat body PLIN1A and B mRNA levels in the larva of the last instar and adults were profiled by qPCR using primers specific to each isoform (exon 1A and 1B) as described in Materials and Methods. In the feeding larva, PLIN1B mRNA levels were higher than those of the variant A and reached a maximum on day 3 when PLIN1B doubled the abundance of PLIN1A (Fig. 5). Subsequently, PLIN1B mRNA declined during prepupal period (wandering, non-feeding) (Fig. 5). In contrast, PLIN1A mRNA levels were relatively low in the feeding larva but sharply increased (~18-fold higher than PLIN1B) at the onset of the pre-pupal period (day 6 or day 1 of wandering). Afterwards, PLIN1A levels declined prior to pupation (day 9) (Fig. 5) and remained very low during pupal stage (not shown). Subsequently, the onset of adult life was also marked by a high increase in PLIN1A mRNA levels, which were up to ~40-fold over the levels of PLIN1B mRNA (Fig. 5).

In addition to mRNA levels specific to each isoform, mRNA levels of total PLIN1 were also determined. A well conserved region of PLIN1 protein was used to design primers to quantify the totality of PLIN1 transcripts. The targeted region for qPCR amplification encoded amino acids 259 to 306 of PLIN1B protein (Fig. 4B). The corresponding primer sequences corresponding to exon 5 (forward primer) and exon 6 (reverse primer) are provided in Materials and Methods. As it can be seen in Fig. 5, the mRNA levels of total PLIN1 in the adult fat body were very similar to the levels of PLIN1A mRNA indicating that PLIN1A was the predominant isoform present in that period. However, in the 5th feeding larva, total PLIN1 mRNA levels were similar to the sum of the corresponding PLIN1A and B levels implying that these two transcripts comprise the majority of fat body PLIN1 mRNA. As mentioned above, the predicted proteins encoded by these transcripts have molecular weights of 41.8 kDa (PLIN1A) and 47.9 kDa (PLIN1B). The fact that these two isoforms were the only PLIN1 proteins detected by Western blot (Fig. 1) is in agreement with the fact that these two transcripts were also the predominant variants detected by qPCR (Fig. 5).

According to the gene structure depicted in Fig. 3, the alternative usage of different promoters would explain the occurrence of these two transcripts. Moreover, the changes in the transcript levels during development (e.g. exon 1B transcript was increased in the feeding larvae whereas exon 1A transcript was increased at the onset of pre-pupal and adult stages (Fig. 5) suggest the involvement of developmental cues in the regulation of PLIN1 gene expression.

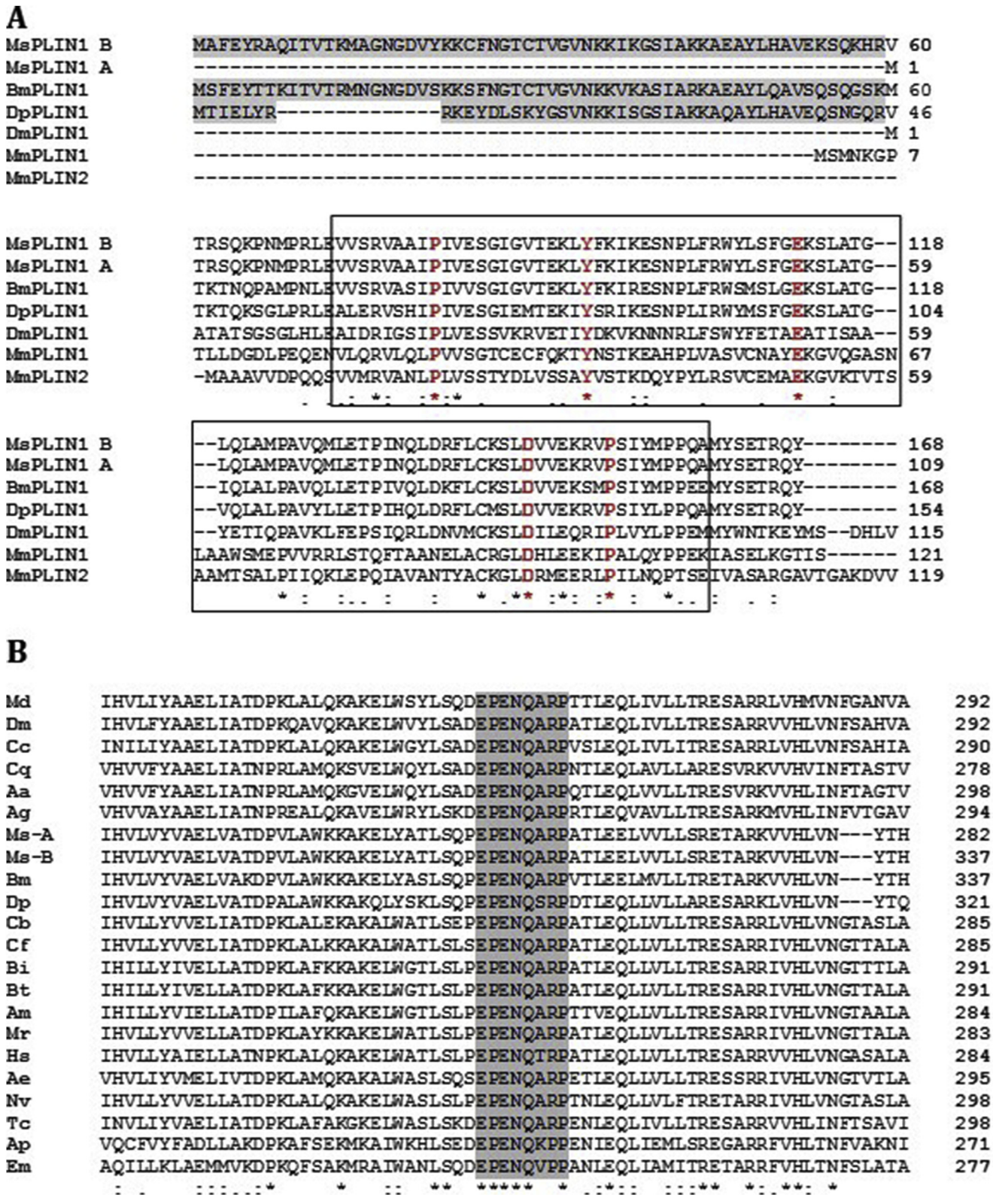

(caption on next page)

3.4. PLIN1 protein abundance in the 5th larval instar fat body

PLIN1B levels throughout 5th instar larval development were determined by immunoblot of LD proteins (Fig. 6A–B). We have previously reported that in SDS-PAGE analysis of LD proteins from adult fat body, PLIN1 runs as a doublet (Patel et al., 2005). PLIN1 also runs as a doublet in the larval fat body. The reason for the presence of a doublet is unknown. PLIN1B was almost undetected in very young larvae but gradually increased along the feeding phase reaching its maximum on day 5 (Fig. 6 A). PLIN1B gradually declined during the pre-pupal stage (Fig. 6 B). The changes in the PLIN1B/PLIN1 A ratio during the 5th instar are shown in Fig. 6 C and D. In the feeding larva, PLIN1B levels

Fig. 4. Multiple alignment analysis of insect PLIN1 proteins and vertebrate PLIN proteins. A) Alignment of the deduced amino acid sequence of perilipins from *M. sexta* (MsPLIN1B, AIE17454.1; MsPLIN1A, AIE17453.1), *D. melanogaster* (DmPLIN1, AAF56183.2), *B. mori* (BmPLIN1, NP_001040143.1), *D. plexippus* (DpPLIN1, EHJ65253.1), mouse PLIN1 A (MmPLIN1, NP_001106942.1), and mouse PLIN2 (MmPLIN2, NP_031434.3). ClustalW2 (http:www.ebi.ac.uk/Tools/msa/clustalw2/) was used for the alignments. The putative PAT domain originally described for vertebrate perilipin is framed (Lu et al., 2001). The five amino acids of the PAT domain (P, Y, E, D, P) that are 100% identical in 22 insect PLIN1 and 8 vertebrate PLIN sequences are highlighted in bold. **B)** Alignment of PLIN1 sequence regions containing the putative membrane-binding motif from 22 insect PLIN1 sequences. The highly conserved ^{304}EPENQARP^{311} sequence is shaded. *Abbreviations and sequence identifiers: Md, Musca domestica, XP_005189534.1; Dm, Drosophila melanogaster, NP_651183; Cc, Ceratitis capitata, XP_004523385.1; Cq Culex quinquefasciatus, XP_001845547.1; Aa, Aedes aegypti, XP_021693334.1; Ag, Anopheles gambiae, XP_312022.5; Cb, Coceraea biroi, EZA55190.1;* Cf, *Camponotus floridanus, EFN73399.1; Bi, Bombus impatiens, XP_003486284.1; Bt, Bombus terrestris, XP_012167204.1; Am, Apis mellifera, XP_026298733.1; Mr, Megachile rotundata, XP_012140334.1; Hs, Harpegnathos saltator, EFN86122.1; Ae, Acromyrmex echinatior, XP_011061820.1; Nv, Ceratosolen solmsi marchali, XP_011497754.1; Tc, Tribolium castaneum, EEZ98760.2; Ap, Acyrthosiphon pisum, XP_003240113.3; Em, Eurygaster Maura, AHA90810.1.*

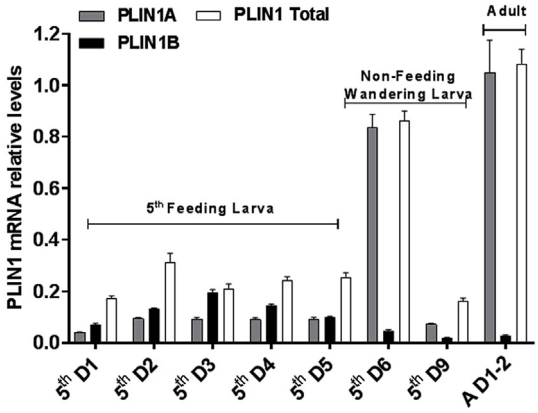

Fig. 5. PLIN1 mRNA level during development. mRNA was isolated from fat bodies of 5th instar feeding larvae (day 1–5), non-feeding wandering larvae (day 6 and 9), and adults (day 1–2). PLIN1 mRNA levels were determined by qPCR using primers targeting PLIN1A (grey bar) and PLIN1B (black bar) specific exons as well as the internal (clear bar) common region between both PLIN1 isoforms. All mRNA levels were normalized to mRNA ribosomal protein S3. At least two independent sets of total RNA were analyzed in triplicate and relative values are plotted as the mean ± SD.

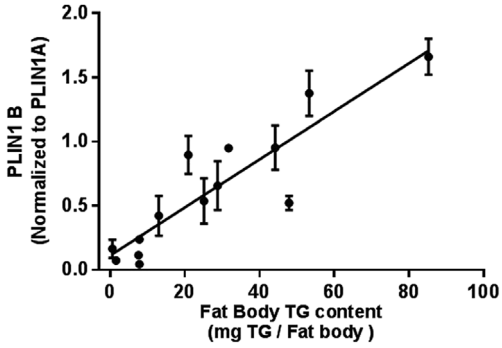

Fig. 7. PLIN1B expression correlates with lipid storage in 5th instar larva during feeding. The plot shows PLIN1B abundance (normalized to the content of PLIN1A) and the fat body TG content (mg TG/fat body) from day 1 through 5 in insects of the 5th instar feeding period. The correlation coefficient (r^2) of the linear regression was 0.8141, $p < 0.0001$.

closely followed the changes in TG storage (Fig. 6 C). In fact, PLIN1B abundance normalized to PLIN1A directly correlated with TG content suggesting a relationship between the increase in TG storage and PLIN1B in the fat body of the 5th instar (Fig. 7). In addition, Fig. 6 C shows PLIN2 levels along development (day 1–5). These levels previously reported were included in Fig. 6 C to facilitate the reading (Chen et al., 2017). The accumulation of lipids in the first phase (day 1–3) was followed by both PLIN2 and PLIN1B. However, at the time of maximal TG accumulation (days 3–5), the levels of MsPLIN2 declined and remained very low in subsequent larval development (Chen et al., 2017). This unexpected finding suggested the occurrence of alternative mechanism/s to shield TG from the action of lipases in *M. sexta* LDs. Here, we uncovered a novel PLIN1 isoform -PLIN1B-, which could take PLIN2 role as a barrier to lipases when cellular TG content is high.

During the subsequent non feeding phase, PLIN1 B declined (shown in Fig. 6 C) and fat body lipids were secreted to the hemolymph (shown in Fig. 6 D). Thus, the decline of PLIN1B/PLIN1A ratio during the pre-

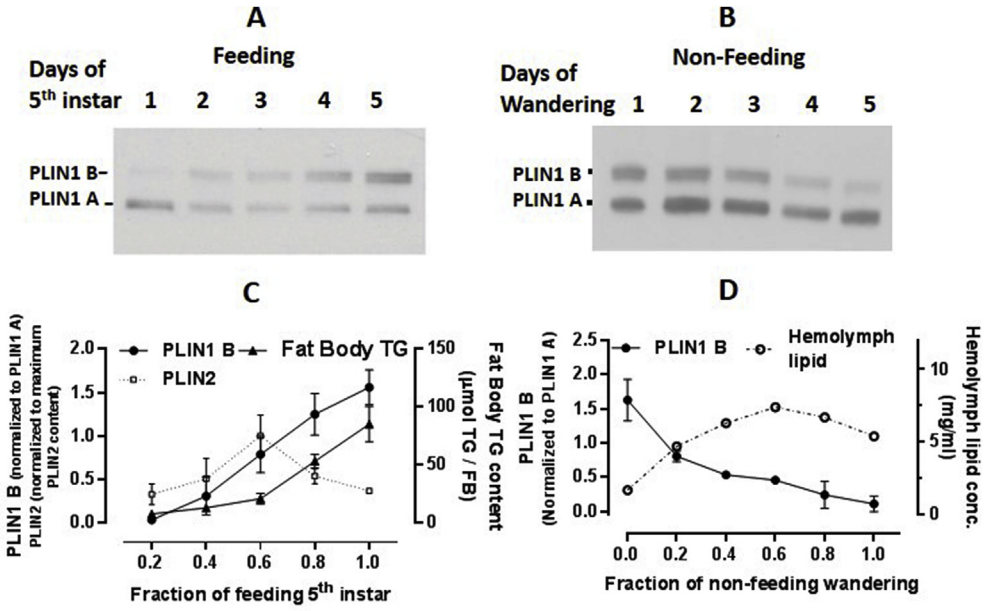

Fig. 6. Expression of PLIN1 in the fat body of 5th instar *M. sexta*. A-B) Western blots of LDs proteins (20 µg) from the fat bodies of: **A)** feeding larvae (days 1–5) and **B)** non-feeding or wandering larvae (days 6–10); **C)** PLIN1B, PLIN2 and TG content in the fat body of feeding larvae: PLIN1B abundance was calculated by densitometry of the immunoblots and normalized to PLIN1A; PLIN2 abundance was normalized to PLIN2 maximal value; TG content is expressed in µmol TG/fat body (mean ± SD, n = 3). **D)** Changes in PLIN1B and hemolymph lipid concentration during the non-feeding larval stage prior to pupation: PLIN1B abundance was calculated and expressed as in C). Each day of the feeding larvae and prepupal period (wandering) represents 0.2 (20%) of the total feeding period or the wandering period, respectively.

pupal period coincided with the mobilization of fat body lipids to the hemolymph. While the abundance of PLIN1B during feeding (days 1–5) followed the accumulation of TG in the fat body (Fig. 6 C), the PLIN1B decrease and PLIN1A increase during the non-feeding phase coincided with the mobilization of lipids to the hemolymph (Fig. 6 B and D).

On the other hand, PLIN1A levels were less abundant than that of PLIN1B in the feeding larvae except on day 1 coming out of the molt. In the second day, PLIN1A levels decreased and remained relatively low during the feeding phase (Fig. 6 A). However, at the onset of the pre-pupal non-feeding period, PLIN1A increased significantly (Fig. 6 B) and this increase coincided with mobilization of lipids to the hemolymph (Fig. 6 D). PLIN1A strong expression in pre-pupal insects was consistent with its proven role in lipolysis. In contrast, PLIN1B expression that occurred during the feeding period accompanied lipid accumulation. In view of these data, PLIN1B does not seem to play a role in lipid mobilization as PLIN1A. Despite the fact that PLIN1B is a larger version of PLIN1A, these proteins seem to have opposite roles in terms of TG storage.

The cellular level of lipid storage could be modulating the expression of exon 1B transcript of PLIN1. However, we did not find total correspondence between PLIN1A and B mRNA and protein levels (Figs. 5 and 6). The high level of PLIN1A mRNA at the onset of pre-pupal and adult stages (Fig. 5) corresponded with a higher content of PLIN1A protein (Figs. 6 B and Fig 1). However, the maximum content of PLIN1B protein (day 5 of the feeding larva, Fig. 6 A and C) did not correspond with the highest mRNA level of exon 1B transcript that happened on day 3 of the feeding larva (Fig. 5). The lack of correspondence suggests that other mechanism beyond transcriptional levels could be involved in the fine tuning providing the right cellular level of PLIN1 B protein.

3.5. PLIN1 B levels and TG storage

PLIN1B content in the lipid droplets correlated with TG storage along the 5th instar development (Fig. 7). To test whether this relationship is determined by the accumulation of lipids or by developmental cues (Nijhout et al., 2014), we analyzed the expression of PLIN1B in insects of the same age but differing in the fat body TG content. 5th instar larvae with different levels of fat reserves were produced by feeding the animals with diets of different caloric content (leaves, leaves covered with vegetable oil, artificial diet and artificial diet mixed with oil). Insects were kept and fed in individual cups from day 1 of the 5th instar. On day 3, fat bodies were collected and analyzed for lipid content, LD sizes, and PLIN1 levels (Fig. 8). The content of lipids varied significantly among the groups. Insects on leaf diet had 0.33 ± 0.06 mg TG/fat body whereas in animals fed on leaves plus oil the TG content reached 13.4 ± 1.1 mg TG/fat body. On the other hand, in animals fed the standard diet without and with oil the TG content was 21.0 ± 1.7 and 41.8 ± 6.1 mg TG/fat body, respectively. The average size of the LDs seemed to increase with the caloric content of the diet (Fig. 8A–D). For example, the fat bodies from animals fed on leaves displayed LDs of 1.90 ± 0.77 μm (n = 157) whereas the average size increased to 4.34 ± 2.66 μm (n = 202) when oil was added to the leaves (Fig. 8 B). Likewise, average LD sizes of 6.29 ± 2.59 μm (n = 139) and 7.10 ± 2.86 μm (n = 153) were estimated in the fat bodies from animals fed on the artificial diet (Fig. 8 C) and diet supplemented with oil (Fig. 8 D), respectively. To better understand the loading of TG in the fat body cell under the different conditions, the LD diameters were arranged in two groups -small LD (diameter ≤ 5 μm) and large LD (diameter > 5.5 μm)- and the distribution of LD counts in each group was estimated. Data are shown in Fig. 8 E. In the fat body of insects fed on leaves lipids were packed only in small LDs (100%). However, when leaves were mixed with oil, the total content of fat body lipids increased from less than 1 mg up to 13 mg TG/fat body and the amount of larger droplets (> 5.5 μm) increased to ~35% whereas the small LDs decreased to 64.8 ± 8%. Insects fed on the artificial diet accumulated the largest amount of lipids in their fat bodies and also displayed greater populations of large LDs than those fed on leaves. Moreover, insects fed on the artificial (standard) diet with oil showed the greatest population of large LDs (77 ± 10.8 vs. 67.9 ± 14.6% with no oil). Estimation of PLIN1B by Western blot showed that this isoform was more abundant in the fat body that displayed greater proportion of large size LDs. Moreover, its abundance gradually increased with the increase of the caloric content of the diet. Although PLIN1 A protein also increased with the caloric content of the diet, the most notorious change was between insects fed on leaves and the rest of the feeding conditions. These data suggest that once PLIN1A reaches a threshold level (seen here in Leaf plus oil diet) further lipid accumulation affects PLIN1B abundance, which keeps increasing unlike PLIN1A. These data add support to the notion that the appearance of PLIN1B in the fat body increases with the accumulation of lipids, and probably the presence of large LD. Although we consistently observed that the larval fat body tissue with more content of lipid storage also has larger droplets, the limitations of microscopy due to the fixation process cannot be completely excluded in these experiments.

To further explore the relationship between PLIN1 and TG accumulation in the larval fat body, we analyzed PLIN1 expression of starved insects and insects in which TG storage was restored by re-feeding. Second day 5th instar larvae (fed day 2) were starved for 24 h and then re-fed for 2 h, 6 h, 24 h, and 48 h. Fat body tissue that was collected after each period (fed day 2, 0 h (24 h starvation), 2 h, 6 h, 24 h, and 48 h). Starvation decreased the TG content of the fat body to 8.49 ± 0.98 mg (~35% decrease). After 48 h re-feeding the fat body gained ~39.4 mg of TG. PLIN1 levels were determined by Western blot and qPCR. mRNA levels of diacylglycerol-acyltransferase (DAGT), the enzyme catalyzing the last step in the synthesis of TG, were used to monitor lipid synthesis after re-feeding (Soulages et al., 2015). Likewise, given the role of PLIN2 in lipid accumulation in the larvae of *M. sexta,* mRNA levels of PLIN2 were also included. During 24 h starvation, both mRNA and protein PLIN2 levels markedly decreased (Chen et al., 2017). As it can be seen in Fig. 9 A, starvation promoted a significant decrease in the mRNA levels of PLIN1A (~50% decrease), PLIN1B (~70% decrease), PLIN2 and DGAT. As expected, following re-feeding the lipid synthesis was gradually restored as judged by the gradual increase in DGAT mRNA levels (Fig. 9 A). As previously shown, PLIN2 mRNA increases with lipid synthesis (DGAT) to a point, which in these experiments was around 6 h after re-feeding, and afterwards, lipid synthesis continued on the rise, while PLIN2 mRNA levels reached a plateau and PLIN1B mRNA increased. Unlike PLIN2, the levels of PLIN1 proteins remained relatively stable during the 24 h starvation period (Fig. 9 B and 9 S). Fig. 9 B shows that PLIN1B protein increases during re-feeding and it surpasses the levels of PLIN1 A after 24 h of re-feeding. The changes in levels of PLIN1 A and B are shown in Fig. 9 C.

4. Discussion

Animals have evolved to regulate the storage and mobilization of TG by conserved mechanisms involving the Perilipin family of lipid droplet-associated proteins (Sztalryd and Brasaemle, 2017). PLIN proteins are found in all animals, yet the repertoire in insect is not as complex as in vertebrates (Kuhnlein, 2011). Both PLIN1 and 2 of insects have been associated with TG metabolism in the fat body, however the study of these proteins is in early stages (Arrese et al., 2014). A new PLIN1 isoform -MsPLIN1B- was uncovered in the fat body of the 5th instar of the tobacco hornworm (Figs. 1–6 A and B) and the finding was confirmed by the cDNA cloning and mass spectrometry (Fig. 3S A-B, 6S A and B) of the lipid droplets-associated proteins. The information was consistent with the *Manduca* PLIN1 gene sequence (Kanost et al., 2016). The gene consists of 10 exons and two transcriptional start sites, which are most likely controlled by the usage of alternative promoters (Fig. 3). Alternative transcripts A and B -differing in the alternative use of exon 1 (A and B) - were the most abundant PLIN1 transcripts in the fat body

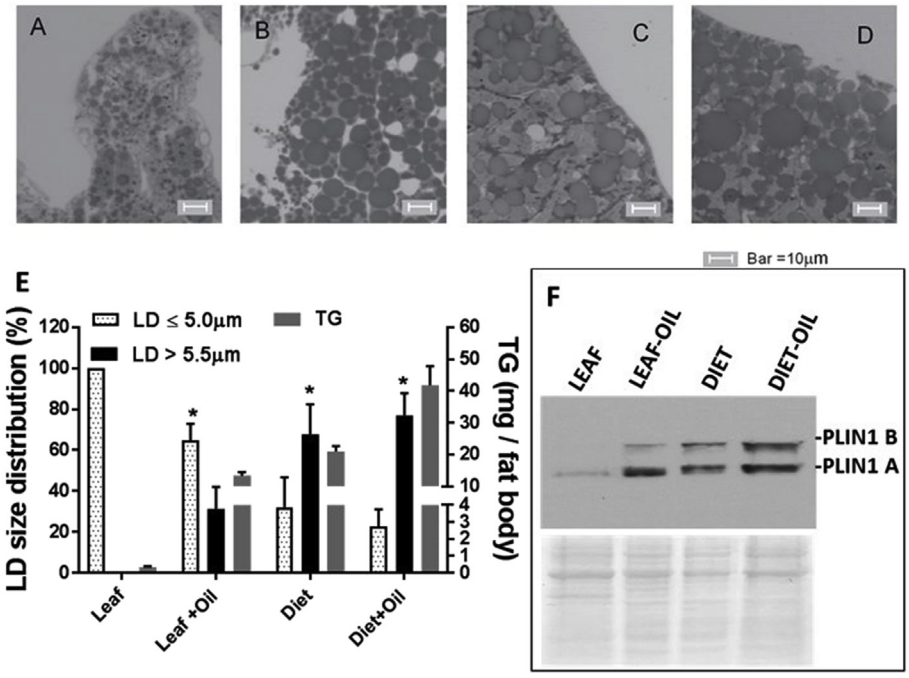

Fig. 8. PLIN1B content increases with the size of lipid droplets in the fat body of 5th instar larvae. **A-D)** Microscopy images of fat body from 5th instar larva fed on different diets: A-Leaves, B-Leaves with oil, C- Standard Diet, D- Diet with oil. **E)** Distribution of LDs sizes in samples A to D: LD sizes were clustered in two classes (≤5 μm and > 5.5 μm) according to their diameters. Dotted bars and black bars depict values (mean % ± SD) corresponding to samples shown in A, B, C and D, respectively. The means for small and large LDs within each group were compared by Student t-test. Corresponding *p* values were < 0.001, < 0.005, and < 0.0001 for the comparisons in B, C, and D groups, respectively. **F)** Western blot analysis of PLIN1 expression in lipid droplets isolated from fat bodies of larvae fed on different diets (Top panel). The Ponceau staining of the membrane is shown in the lower panel.

(Fig. 4). Both transcripts were present at varying levels throughout development (Fig. 5) but at the protein level, PLIN1B was confined to the 5th instar (Figs. 1 and 6 A and B).

Since PLIN1 B was absent in adult of *M. sexta*, we carried out a series of studies in 5th instar larva to gain information on its role. The 5th instar larva of *M. sexta* raised in the lab is characterized by the fast growth during this 5-day period in which the animals accumulate 90% of the maximal mass reached during their lifetime (Nijhout et al., 2006). Likewise, fat reserves increases ~10-fold as compared to the 4th instar larva (Chen et al., 2017). The accumulation of lipids parallels the increase in LD size especially from the 3rd day when the LD enlargement is unmistakable and there is a 4-fold increase in the TG content of fat body (Chen et al., 2017). PLIN2 has been associated to TG storage in *Drosophila* (Grönke et al., 2003) and in *Manduca* (Chen et al., 2017). But in *Manduca* PLIN2 accompanied the accumulation of lipids during the 5th instar development only when TG was packed in small droplets, at the beginning of the instar (days 1–3) while the huge TG accumulation that takes place on days 4 and 5 was accompanied by a decline in PLIN2 protein levels (Chen et al., 2017). The results showed here suggest that PLIN1B, whose abundance normalized to PLIN1A correlated with TG storage (Fig. 7) and the apparent increase in the size of LD (Fig. 9), could take the purported role of PLIN2, shielding TG in the growing droplets. It can be inferred from results shown in this study and the report on MsPLIN2 (Chen et al., 2017) that both proteins, PLIN2 and PLIN1B, are involved in the process of lipid accumulation. The interplay in the expression pattern of these proteins is reminiscent to the process in adipocyte maturation in vertebrates, in which PLIN1 replaces PLIN2 when droplets achieve a significant size (Brasaemle et al., 1997; Souza et al., 2002).

The analysis of PLIN1 expression in the pre-pupal period (non-feeding) - when feeding ceases and the fat body switches from TG storage (Fig. 6 C) to TG mobilization (Fig. 6 D)- was consistent with a role of PLIN1A in lipolysis, and a role of PLIN1B in lipid storage (Fig. 6). The sharp increase of PLIN1A mRNA levels at the onset of the non-feeding period (Fig. 6) leads to newly synthesized PLIN1A (Fig. 7B), which localizes to LDs. In turn, droplets coated with PLIN1A would engage in lipolysis for lipid secretion as indicated in previous studies (Patel et al., 2005; Arrese et al., 2008a). The quick appearance of

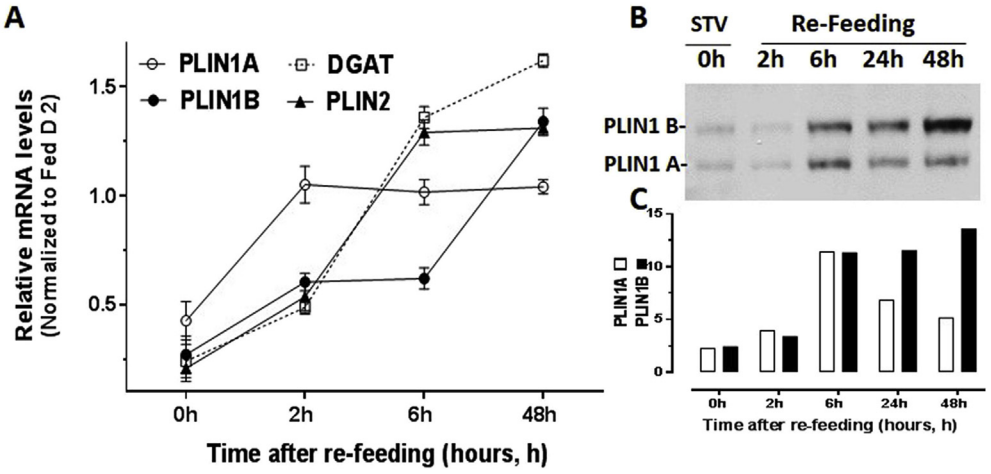

Fig. 9. Effect of starvation and refeeding in the expression of PLIN1 in the fat body of 5th instar larvae Total RNA and LDs were obtained from the fat body of at least three insects. Fed 5th larvae, day 2 (FED), was subjected to 24 h starvation (STV). The end of STV was labeled as 0 h. Refeeding of starved larvae was allowed for 2 h, 6 h and 48 h. **A)** mRNA Levels: The relative levels of PLIN1A, PLIN1B, PLIN2 and DGAT mRNA were determined by qPCR using mRNA RpS3 as reference. Relative values were normalized to the fed state, day 2 (Fed, D 2). The assay was performed by triplicate and the relative values are plotted as the mean ± SD. **B)** Representative Western blot image obtained with 20 μg of LDs proteins for fat bodies of starved (STV), and re-fed (2 h, 6 h and 48 h) insects. **C)** Densitometry of the immunoblot, PLIN1A (clear bars), PLIN1B (black bars).

PLIN1A at the onset of pre-pupal stage when the fat body secretes lipids to the hemolymph further suggests that PLIN1A is required for lipolysis and lipid secretion, but also that PLIN1B is not involved in lipid mobilization.

The mobilization of lipids to the hemolymph in adult *Manduca* is even higher than during the pre-pupal stage. For example, the hemolymph lipid concentration in wandering insects is 7 mg/ml whereas in the adults is 45 mg/l (Tsuchida and Wells, 1988; Ziegler, 1991). The fat body of adults has the highest content of PLIN1A and lacks PLIN1B (Arrese et al., 2008b; Soulages et al., 2012). In addition, it has the highest content of TGL, the main cytosolic lipase (Arrese et al., 2010). The lipolytic rate of adult fat body is 9-fold higher than the rate of the 5th instar larva fat body, which has the lowest fat body lipolytic activity (Arrese et al., 2010) and the highest proportion of PLIN1B (Fig. 1). The combination of these factors -PLIN1B abundance and lipolysis rate-explains the high accumulation of fat body lipids at the end of the last feeding period prior to pupation as it is shown in Fig. 6 C.

Lastly, while PLIN1A was present in all insect genomes so far, isoform B occurred only in lepidopteran species (Figs. 4 and 10 S). The order Lepidoptera (moths and butterflies) is the second large group of insects including more than 150,000 species (Powell, 2003). Caterpillars are characterized for having a voracious appetite particularly the older larvae, which can be very destructive. Given that PLIN1B was expressed only in the older tobacco hornworms when they were accumulating massive amounts of fat reserves, one can speculate that PLIN1B of caterpillars reinforces the ability of the fat body to store TG just prior to pupation. Here we uncovered a novel PLIN1 isoform whose expression, unlike PLIN1A, was associated with TG storage. The study provides insight into the dual role of PLIN1 gene of lepidoptera in the fundamental processes of TG storage and mobilization.

Acknowledgements

This project was supported by Oklahoma Agricultural Experiment Station (OKL02398), Oklahoma State University and by Grant Number R01GM064677 from the National Institute of General Medical Sciences. The content is solely the responsibility of the authors and does not necessarily represent the official use of the National Institute of General Medical Sciences or the National Institutes of Health. The authors are grateful to Janet Rogers and Lisa Whitworth for their excellent technical assistance in the experiments of mass spectrometry and microscopy, respectively.

Appendix A. Supplementary data

Supplementary data to this article can be found online at https://doi.org/10.1016/j.ibmb.2019.05.001.

References

Arrese, E.L., Soulages, J.L., 2010. Insect fat body: energy, metabolism, and regulation. Annu. Rev. Entomol. 55, 207–225.
Arrese, E.L., Wells, M.A., 1997. Adipokinetic hormone-induced lipolysis in the fat body of an insect, *Manduca* sexta: synthesis of sn-1,2-diacylglycerols. J. Lipid Res. 38, 68–76.
Arrese, E.L., Rivera, L., Hamada, M., Mirza, S., Hartson, S.D., Weintraub, S., Soulages, J.L., 2008a. Function and structure of lipid storage droplet protein 1 studied in lipoprotein complexes. Arch. Biochem. Biophys. 473, 42–47.
Arrese, E.L., Mirza, S., Rivera, L., Howard, A.D., Chetty, P.S., Soulages, J.L., 2008b. Expression of lipid storage droplet 1 may define the role of AKH as lipid mobilizing hormone in *Manduca sexta*. Insect Biochem. Mol. Biol. 38, 993–1000.
Arrese, E.L., Howard, A.D., Patel, R.T., Rimoldi, O.J., Soulages, J.L., 2010. Mobilization of lipid stores in *Manduca* sexta: cDNA cloning and developmental expression of fat body triglyceride lipase, TGL. Insect Biochem. Mol. Biol. 40, 91–99.
Arrese, E.L., Saudale, F.Z., Soulages, J.L., 2014. Lipid droplets as signaling platforms linking metabolic and cellular functions. Lipid Insights 7, 7–16.
Bell, R.A., Joachim, F.G., 1976. Techniques for rearing laboratory colonies of tobacco hornworms and pink bollworms. Ann. Entomol. Soc. Am. 69, 365–373.
Beller, M., Riedel, D., Jansch, L., Dieterich, G., Wehland, J., Jackle, H., Kuhnlein, R.P., 2006. Characterization of the *Drosophila* lipid droplet subproteome. Mol. Cell. Proteomics : MCP 5, 1082–1094.
Beller, M., Bulankina, A.V., Hsiao, H.H., Urlaub, H., Jackle, H., Kuhnlein, R.P., 2010. PERILIPIN-dependent control of lipid droplet structure and fat storage in *Drosophila*. Cell Metabol. 12, 521–532.
Bi, J., Xiang, Y., Chen, H., Liu, Z., Grönke, S., Kuhnlein, R.P., Huang, X., 2012. Opposite and redundant roles of the two *Drosophila* perilipins in lipid mobilization. J. Cell Sci. 125, 3568–3577.
Bickel, P.E., Tansey, J.T., Welte, M.A., 2009. PAT proteins, an ancient family of lipid droplet proteins that regulate cellular lipid stores. Biochim. Biophys. Acta 1791, 419–440.
Biochim BiophysDucharme, N.A., Bickel, P.E., 2008. Lipid droplets in lipogenesis and lipolysis. Endocrinology 149, 942–949.
Brasaemle, D.L., 2007. Thematic review series: adipocyte biology. The perilipin family of structural lipid droplet proteins: stabilization of lipid droplets and control of lipolysis. J. Lipid Res. 48, 2547–2559.
Brasaemle, D.L., Barber, T., Wolins, N.E., Serrero, G., Blanchette-Mackie, E.J., Londos, C., 1997. Adipose differentiation-related protein is an ubiquitously expressed lipid storage droplet-associated protein. J. Lipid Res. 38, 2249–2263.
Brasaemle, D.L., Rubin, B., Harten, I.A., Gruia-Gray, J., Kimmel, A.R., Londos, C., 2000. Perilipin A increases triacylglycerol storage by decreasing the rate of triacylglycerol hydrolysis. J. Biol. Chem. 275, 38486–38493.
Canavoso, L.E., Jouni, Z.E., Karnas, K.J., Pennington, J.E., Wells, M.A., 2001. Fat metabolism in insects. Annu. Rev. Nutr. 21, 23–46.
Cermelli, S., Guo, Y., Gross, S.P., Welte, M.A., 2006. The lipid-droplet proteome reveals that droplets are a protein-storage depot. Curr. Biol. 16, 1783–1795.
Chen, X., Firdaus, S.J., Howard, A.D., Soulages, J.L., Arrese, E.L., 2017. Clues on the function of *Manduca sexta* perilipin 2 inferred from developmental and nutrition-dependent changes in its expression. Insect Biochem. Mol. Biol. 81, 19–31.
Chen, X., Goodman, J.M., 2017. The Collaborative Work of Droplet Assembly.
Folch, J., Lees, M., Stanley, G.H.S., 1957. A simple method for the isolation and purification of total lipides from animal tissues. J. Biol. Chem. 226, 497–509.
Gramates, L.S., Marygold, S.J., Santos, G.D., Urbano, J.M., Antonazzo, G., Matthews, B.B., Rey, A.J., Tabone, C.J., Crosby, M.A., Emmert, D.B., Falls, K., Goodman, J.L., Hu, Y., Ponting, L., Schroeder, A.J., Strelets, V.B., Thurmond, J., Zhou, P., the FlyBase Consortium, 2017. FlyBase at 25: looking to the future. Nucleic Acids Res. 45 (D1), D663–DD671.
Grönke, S., Beller, M., Fellert, S., Ramakrishnan, H., Jackle, H., Kuhnlein, R.P., 2003. Control of fat storage by a *Drosophila* PAT domain protein. Curr. Biol. 13, 603–606.
Hodges, B.D., Wu, C.C., 2010. Proteomic insights into an expanded cellular role for cytoplasmic lipid droplets. J. Lipid Res. 51, 262–273.
Kanost, M.R., Arrese, E.L., Cao, X., Chen, Y.R., Chellapilla, S., Goldsmith, M.R., Grosse-Wilde, E., Heckel, D.G., Herndon, N., Jiang, H., Papanicolaou, A., Qu, J., Soulages, J.L., Vogel, H., Walters, J., Waterhouse, R.M., Ahn, S.J., Almeida, F.C., An, C., Aqrawi, P., Bretschneider, A., Bryant, W.B., Bucks, S., Chao, H., Chevignon, G., Christen, J.M., Clarke, D.F., Dittmer, N.T., Ferguson, L.C., Garavelou, S., Gordon, K.H., Gunaratna, R.T., Han, Y., Hauser, F., He, Y., Heidel-Fischer, H., Hirsh, A., Hu, Y., Jiang, H., Kalra, D., Klinner, C., Konig, C., Kovar, C., Kroll, A.R., Kuwar, S.S., Lee, S.L., Lehman, R., Li, K., Li, Z., Liang, H., Lovelace, S., Lu, Z., Mansfield, J.H., McCulloch, K.J., Mathew, T., Morton, B., Muzny, D.M., Neunemann, D., Ongeri, F., Pauchet, Y., Pu, L.L., Pyrousis, I., Rao, X.J., Redding, A., Roesel, C., Sanchez-Gracia, A., Schaack, S., Shukla, A., Tetreau, G., Wang, Y., Xiong, G.H., Traut, W., Walsh, T.K., Worley, K.C., Wu, D., Wu, W., Wu, Y.Q., Zhang, X., Zou, Z., Zucker, H., Briscoe, A.D., Burmester, T., Clem, R.J., Feyereisen, R., Grimmelikhuijzen, C.J., Hamodrakas, S.J., Hansson, B.S., Huguet, E., Jermiin, L.S., Lan, Q., Lehman, H.K., Lorenzen, M., Merzendorfer, H., Michalopoulos, I., Morton, D.B., Muthukrishnan, S., Oakeshott, J.G., Palmer, W., Park, Y., Passarelli, A.L., Rozas, J., Schwartz, L.M., Smith, W., Southgate, A., Vilcinskas, A., Vogt, R., Wang, P., Werren, J., Yu, X.Q., Zhou, J.J., Brown, S.J., Scherer, S.E., Richards, S., Blissard, G.W., 2016. Multifaceted biological insights from a draft genome sequence of the tobacco hornworm moth, *Manduca sexta*. Insect Biochem. Mol. Biol. 76, 118–147.
Kimmel, A.R., Brasaemle, D.L., McAndrews-Hill, M., Sztalryd, C., Londos, C., 2010. Adoption of PERILIPIN as a unifying nomenclature for the mammalian PAT-family of intracellular lipid storage droplet proteins. J. Lipid Res. 51, 468–471.
Kuhnlein, R.P., 2011. The contribution of the *Drosophila* model to lipid droplet research. Prog. Lipid Res. 50, 348–356.
Law, J.H., Wells, M.A., 1989. Insects as biochemical models. J. Biol. Chem. 264, 16335–16338.
Lin, P., Chen, X., Moktan, H., Arrese, E.L., Duan, L., Wang, L., Soulages, J.L., Zhou, D.H., 2014. Membrane attachment and structure models of lipid storage droplet protein 1. Biochim. Biophys. Acta 1838 (3), 874–881.
Livak, K.J., Schmittgen, T.D., 2001. Analysis of relative gene expression data using real-time quantitative PCR and the 2(-Delta Delta C(T)) Method. Methods 25 (4), 402–408.
Lu, X.Y., Gruia-Gray, J., Copeland, N.G., Gilbert, D.J., Jenkins, N.A., Londos, C., Kimmel, A.R., 2001. The murine perilipin gene: the lipid droplet-associated perilipins derive from tissue-specific, mRNA splice variants and define a gene family of ancient origin. Mamm. Genome 12, 741–749.
Martinez-Botas, J., Andreson, J., Tessler, D., Lapilojnne, B., Hung-Junn Chang, B., Quast, M., Gorenstein, D., Chen, K.H., Chan, L., 2000. Absence of perilipin results in leanness and reverses obesity in Leprdb/db mice. Nat. Genet. 26, 474–479.
Miura, S., Gan, J.W., Brzostowski, J., Parisi, M.J., Schultz, C.J., Londos, C., Oliver, B., Kimmel, A.R., 2002. Functional conservation for lipid storage droplet association among Perilipin, ADRP, and TIP47 (PAT)-related proteins in mammals, *Drosophila*, and *Dictyostelium*. J. Biol. Chem. 277, 32253–32257.
Miyoshi, H., Souza, S.C., Endo, M., Sawada, T., Perfield II, J.W., Shimizu, C., Stancheva, Z., Nagai, S., Strissel, K.J., Yoshioka, N., Obin, M.S., Koike, T., Greenberg, A.S., 2010. Perilipin overexpression in mice protects against diet-induced obesity. J. Lipid Res.

51, 975–982.
Najt, C.P., Lwande, J.S., McIntosh, A.L., Senthivinayagam, S., Gupta, S., Kuhn, L.A., Atshaves, B.P., 2014. Structural and functional assessment of Perilipin 2 lipid binding domains(s). Biochemistry 53, 7051–7066.
Nijhout, H., Davidowitz, G., Roff, D., 2006. A quantitative analysis of the mechanism that controls body size in *Manduca sexta*. J. Biol. 5, 1–15.
Nijhout, H.F., Riddiford, L.M., Mirth, C., Shingleton, A.W., Suzuki, Y., Callier, V., 2014. The developmental control of size in insects. Wires Dev. Biol. 3, 113–134.
Ohnishi, A., Hull, J.J., Kaji, M., Hashimoto, K., Lee, J.M., Tsuneizumi, K., Suzuki, T., Dohmae, N., Matsumoto, S., 2011. Hormone signaling linked to silkmoth sex pheromone biosynthesis involves Ca2+/calmodulin-dependent protein kinase II-mediated phosphorylation of the insect PAT family protein Bombyx mori lipid storage droplet protein-1 (BmLsd1). J. Biol. Chem. 286, 24101–24112.
Patel, R.T., Soulages, J.L., Hariharasundaram, B., Arrese, E.L., 2005. Activation of the lipid droplet controls the rate of lipolysis of triglycerides in the insect fat body. J. Biol. Chem. 280, 22624–22631.
Powell, J.A., 2003. Lepidoptera. In: Resh, V.H., Carde, R.T. (Eds.), Encyclopedia of Insects. Academic Press, New York, pp. 631–664.
Romero-Calvo, I., Ocon, B., Martinez-Moya, P., Suarez, M.D., Zarzuelo, A., Martinez-Augustin, O., de Medina, F.S., 2010. Reversible Ponceau staining as a loading control alternative to actin in Western blots. Anal. Biochem. 401, 318–320.
Soulages, J.L., Firdaus, S.J., Hartson, S., Chen, X., Howard, A.D., Arrese, E.L., 2012. Developmental changes in the protein composition of *Manduca sexta* lipid droplets. Insect Biochem. Mol. Biol. 42, 305–320.
Soulages, J.L., Wu, Z., Firdaus, S.J., Mahalingam, R., Arrese, E.L., 2015. Monoacylglycerol and diacylglycerol acyltransferases and the synthesis of neutral glycerides in *Manduca sexta*. Insect Biochem. Mol. Biol. 62, 194–210.
Souza, S.C., Muliro, K.V., Liscum, L., Lien, P., Yamamoto, M.T., Schaffer, J.E., Dallal, G.E., Wang, X.Z., Kraemer, F.B., Obin, M., Greenberg, A.S., 2002. Modulation of hormone-sensitive lipase and protein kinase A-mediated lipolysis by perilipin A in an adenoviral reconstituted system. J. Biol. Chem. 277, 8267–8272.
Sztalryd, C., Brasaemle, D.L., 2017. The perilipin family of lipid droplet proteins: gatekeepers of intracellular lipolysis. Biochim. Biophys. Acta 1862, 1221–1232.
Tansey, J.T., Sztalryd, C., Gruia-Gray, J., Roush, D., Zeo, J., Gavrilova, O., Reitman, M., Deng, C.X., Ki, C., Kimmel, A.R., 2001. Perilipin ablation results in a lean mouse with aberrant adipocyte lipolysis, enhanced leptin production, and resistance to diet-induced obesity. Proc. Natl. Acad. Sci. U.S.A. 98, 6494–6499.
Tansey, J.T., Sztalryd, C., Hlavin, E.M., Kimmel, A.R., Londos, C., 2004. The central role of perilipin A in lipid metabolism and adipocyte lipolysis. IUBMB Life 56, 379–385.
Toprak, U., Guz, N., Gurkan, M.O., Hegedus, D.D., 2014. Identification and coordinated expression of perilipin genes in the biological cycle of sunn pest, *Eurygaster maura* (Hemiptera: Scutelleridae): implications for lipolysis and lipogenesis. Comp. Biochem. Physiol. B Biochem. Mol. Biol. 171, 1–11.
Tran, T.M., Tran, D.B., Masamitsu, Y., Nguyen, T.H., Kaeko, K., 2016. Function of lipid storage droplet 1 (Lsd1) in wing development of *Drosophila melanogaster*. Int. J. Mol. Sci. 17 (5), 648 2016 May.
Tsuchida, K., Wells, M.A., 1988. Digestion, absorption, transport and storage of fat during the last larval stadium of *Manduca* sexta. Changes in the role of lipophorin in the delivery of dietary lipid to the fat body. Insect Biochem. 18, 263–268.
Van der Horst, D.J., Rodenburg, K.W., 2010. Lipoprotein assembly and function in an evolutionary perspective. Biomol. NMR Assignments 1, 165–183.
Ziegler, R., 1991. Changes in lipid and carbohydrate metabolism during starvation in adult *Manduca sexta*. J. Comp. Physiol. B 161, 125–131.